

Published in final edited form as:

Cancer Res. 2010 February 15; 70(4): 1679–1688. doi:10.1158/0008-5472.CAN-09-2740.

Heterogeneous nuclear ribonucleoprotein H Blocks MST2-Dependent Apoptosis in Cancer Cells via Regulation of A-Raf transcription

Jens Rauch^{1,2}, Eric O'Neill^{2,**}, Brigitte Mack¹, Christoph Matthias³, Markus Munz^{4,***}, Walter Kolch^{2,5,*,#}, and Olivier Gires^{1,4,#}

¹ Department of Head and Neck Research, Ludwig-Maximilians-Universität München, Marchioninstr.15, D-81377 Munich, Germany

² Beatson Institute for Cancer Research, Garscube Estate, Switchback Road, Glasgow G61 1BD, UK.

³ Department of Otorhinolaryngology, University Medicine Göttingen, Robert-Koch-Strasse 40, 37099 Göttingen, Germany.

⁴ Clinical Cooperation Group Molecular Oncology, Department of Head and Neck Research, Ludwig-Maximilians-Universität München, Marchioninstr.15, D-81377 Munich, Helmholtz Zentrum München, German Research Center for Environmental Health, Marchioninstr.25, D-81377 Munich, Germany

⁵ Sir Henry Wellcome Functional Genomics Facility, University of Glasgow, Glasgow G12 8QQ, UK

Summary

A-Raf belongs to the family of oncogenic Raf kinases that are involved in mitogenic signalling by activating the MEK-ERK pathway. Low kinase activity of A-Raf towards MEK suggested that A-Raf might have alternative functions. We show that A-Raf prevents cancer cell apoptosis contingent on the expression of the hnRNP H splice factor, which is required for the correct transcription and expression of A-Raf. A-Raf prevented apoptosis by sequestering and inactivating the pro-apoptotic MST2 kinase. Knock-down of hnRNP H or A-Raf resulted in MST2-dependent apoptosis, while enforced expression of either one partially counteracted apoptosis induced by etoposide. *In vivo* expression studies in colon specimens corroborated the over-expression of hnRNP H in malignant tissues and its correlation with A-Raf levels. In summary, we present a novel route that is usurped by tumor cells to escape naturally imposed apoptotic signals.

Keywords

hnRNP H; apoptosis; A-Raf; splicing; MST2

Correspondence should be addressed to: Olivier Gires Tel.: +49-89-70953895 Fax.: +49-89-70956896 olivier.gires@med.uni-muenchen.de.

*Current address: Systems Biology Ireland, University College Dublin, Dublin 4, Ireland

#These authors are equally contributing senior authors

**Present address: Tumour Suppressor Signalling group, Dept. Radiation Oncology and Biology, University of Oxford, Oxford OX3 7LJ, UK

***Present address: Micromet Inc., Staffelseestr. 2, D-81477 Munich, Germany

Introduction

Heterogeneous nuclear ribonucleoprotein H (hnRNP H) is a member of the subfamily of hnRNPs including hnRNP H, H', F, and 2H9 (1). HnRNP H functions in the splicing of selected target mRNAs such as *c-src* in neuronal cells (2), *Bcl-x* (3, 4), *PLP/DM20* (5), *Drosophila nanos* (6), HIV-1 splicing substrates (7), and rodent tropomyosin (8). According to available knowledge of their functions, hnRNP F/H and hnRNP A/B are key players in alternative splicing (9). As shown more recently, they also have a role in generic splicing, *i.e.* in molecular mechanisms of intron definition (10). Over-expression of hnRNP H was described in various human cancers including hepatocellular, pancreatic, and laryngeal carcinomas (11, 12). Whether and how hnRNP H is linked to the pathogenesis of cancer remains unexplored to date. We combined specific inhibition of hnRNP H expression with whole genome transcriptome analysis, with the aim to analyze the phenotype of hnRNP H-deficient carcinoma cells. High levels of hnRNP H were mandatory for the expression of the full-length A-Raf protein while it impacted neither on Raf-1 nor B-Raf protein expression. Upon knock-down of hnRNP H expression, *a-raf* mRNA levels were reduced. The expression of A-Raf was essential to sequester and deactivate the pro-apoptotic kinase MST2 and inhibit apoptosis. Thus, this study provides a rational explanation for the over-expression of hnRNP H in human tumours as a splicing regulator of the *a-raf* mRNA. In addition, it identifies a role for A-Raf as a potent inhibitor of the MST2 tumour-suppressor pathway in carcinoma cells.

Material and methods

Immunohistochemistry

Carcinoma specimen and healthy tissue were obtained during routine biopsy or surgery after informed consent. Carcinoma and healthy tissues specimen were snap-frozen, cryo-preserved, and processed to generate serial sections (4µm). For immunohistological staining, polyclonal rabbit anti-human hnRNPH antibody (Bethyl Laboratories, Montgomery, US) and polyclonal goat anti-human A-Raf antibody sc-408-G (Santa Cruz, Santa Cruz, US) were used. Antigen-antibody complexes were visualized using the avidin-biotin-PO (ABC) method (13).

Cell lines

HeLa human cervical carcinoma cells, GHD-1 human hypopharynx carcinoma cells, HCT116 human colon carcinoma cells, and HEK293 human embryonic kidney cells were cultured in standard DMEM containing 10% fetal calf serum (FCS) and passaged three times each week. HeLa, HCT116, and HEK293 cell lines were either purchased from ATCC or CRUK. The cells were authenticated by the European Collection of Cell Cultures (ECACC) in September 2009 using microsatellite genotyping (PCR-based). GHD-1 is a self-established cell line from a hypopharynx HNSCC tumour (14).

Laser scanning fluorescence microscopy

Endogenous A-Raf and MST2 expression in HeLa carcinoma cells and human carcinoma specimen was analyzed using a fluorescence laser scanning system (TCS-SP2 scanning system and DM IRB inverted microscope, Leica, Solms, Germany). For A-Raf, MST2, and cytochrome C detection cells were fixed and stained with specific antibodies against A-Raf, MST2, and cytochrome C. Dye-coupled Alexa antibodies (Alexa-488 and Alexa-647; Molecular Probes, Eugene, US) were used as secondary antibodies. Subsequently, Hoechst 33342 was used for labelling of nuclear DNA (Sigma, Taufkirchen, Germany). Leica Confocal Software Lite (Leica, Solms, Germany) for evaluation and quantification was used according to the manufacturer's instructions.

Transfections

Transient transfections of siRNAs and expression plasmids were conducted with MATra-A reagent (IBA, Goettingen, Germany) or the Nucleofector system (amaxa GmbH, Koeln, Germany) according to the manufacturer's instructions. The total amounts of transfected DNA or siRNA was kept constant by filling up with empty vector or control siRNA as required. The following siRNA sequences were used: hnRNPH siRNA#1: 5'-GGAGCUGGCUUUGAGAGGA dTdT-3', siRNA#2: 5'-GAAUAGGGCACAGGUAUUAU dTdT-3', siRNA#3: 5'-GCAAGGAAGAAAUUGUUCA dTdT-3' (Eurogentec, Liège, Belgium), A-Raf: Silencer Validated siRNA 151 (Ambion, Austin, US), MST2: 5'-GGAUAGUUUUUCAAAUAGGdTdT-3', Control siRNA: 5'-UCGUCCGUAUCAUUUCAAU dTdT-3'.

Semi-quantitative RT-PCR

Total RNA from cell lines was isolated using the High Pure RNA Isolation Kit (Macherey & Nagel, Dueren, Germany) and cDNA was generated using the reverse transcription system (Promega, Madison, US) according to the manufacturer's instructions. Total RNA from human tissues was isolated using the RNeasy lysis system (Bertin Technologies, Montigny-le-Bretonneux, France) and the RNeasy Mini Kit (Qiagen, Hilden, Germany) according to the manufacturer's instructions. cDNA was generated using the SuperScript First-Strand Synthesis System for RT-PCR (Invitrogen, Paisley, UK) according to the manufacturer's instructions.

We performed semi-quantitative PCR analysis for the expression of hnRNPH, Bcl-X, A-Raf, GAPDH, and MAPK1 (95 °C for 30 s, annealing for 30 s, 72 °C for 30 s). Amplicon size of the PCR is given in brackets: hnRNPH (385bp): 5'-AAAATGGGGCTCAAGGTATTCG-3', 5'-GCTATTCCTGTGAAGCAAAGTGC-3', A-Raf (210bp): 5'-ATGGAGCCACCACGGGGC-3', 5'-CGTCTTCGTCCTTGATGAGTC-3', Bcl-x (x₁ isoform 456bp, x_s isoform 267bp): 5'-ATGGCAGCAGTAAAGCAAGCG-3', 5'-TCATTTCCGACTGAAGAGTGA-3', GAPDH (258bp): 5'-TGTCGCTCTTGAAGTCAGAGGAGA-3', 5'-AGAACATCATCCCTGCCTCTACTG-3', MAPK1 (233bp): 5'-CCTTCCAACCTGCTGCTCAACAC-3', 5'-GGAAAGATGGGCCTGTTAGAAAGC-3'. ImageJ software (U. S. National Institutes of Health, Bethesda, USA, (15) was used for quantification of RT-PCRs.

Immunoprecipitations

HA-A-Raf was immunoprecipitated using immobilised monoclonal mouse anti-HA tag antibody 3F10 (Roche Diagnostics, Mannheim, Germany). Flag-MST2, flag-A-Raf_{WT} and mutants, flag-Raf-1, and flag-B-Raf were immunoprecipitated using immobilised monoclonal mouse anti-flag antibody M2 (Sigma, Taufkirchen, Germany). Endogenous A-Raf was immunoprecipitated using the polyclonal goat anti-human A-Raf antibody sc-408-G (Santa Cruz, Santa Cruz, US). Endogenous MST2 was immunoprecipitated using the polyclonal goat anti-human MST2 antibody sc-6211 (Santa Cruz, Santa Cruz, US). As an isotype control the polyclonal goat anti-human Enolase antibody sc-7455 (Santa Cruz, Santa Cruz, US) was used. HA-tagged A-Raf was immunoprecipitated using the monoclonal mouse anti-HA antibody 3F10 (Roche Diagnostics, Mannheim, Germany). All antibodies were covalently bound to protein-G sepharose (Amersham, Freiburg, Germany) as described elsewhere (16) in order to avoid interference of immunoglobulin heavy chain bands with the similar sized MST2 protein. Cells were lysed in 10mM TrisHCl pH7.5, 150mM NaCl, 0.5% NP40, supplemented with protease and phosphatase inhibitors (Roche Diagnostics). Lysates were cleared of debris by centrifugation (20,000g, 10') and the supernatant used for

immunoprecipitation. The immunoprecipitates were washed three times with lysis buffer and separated by SDS-PAGE and immunoblotted.

Immunoblot analysis

Protein lysates or immunoprecipitates were resolved by SDS PAGE (10-15%) and blotted on PVDF membrane (Millipore, Bedford, US). Protein visualisation was performed using the following antibodies in combination with HRP-conjugated secondary antibodies and the ECL system (GE-Healthcare, Munich, Germany): Polyclonal rabbit anti-human hnRNPH antibody (Bethyl Laboratories, Montgomery, US), polyclonal goat anti-human A-Raf antibody sc-408-G (Santa Cruz, Santa Cruz, US), polyclonal rabbit anti-human MST2 antibody (Stratagene, La Jolla, US), polyclonal rabbit anti-human Bcl-x₁ antibody (Cell Signalling, Danvers, US), monoclonal mouse anti-human Actin antibody sc-1616 (Santa Cruz, Santa Cruz, US), monoclonal mouse anti-human tubulin antibody sc-8035 (Santa Cruz, Santa Cruz, US), monoclonal mouse anti-human c-Myc antibody sc-40 (Santa Cruz, Santa Cruz, US), monoclonal mouse anti-human Flag antibody F3165 (Sigma, Taufkirchen, Germany), monoclonal mouse anti-human c-Raf-1 antibody 610152 (Becton Dickinson, Franklin Lakes, US), polyclonal rabbit anti-human B-Raf antibody sc-166 (Santa Cruz, Santa Cruz, US), monoclonal rabbit anti-human MST2 (N-term.) antibody 1943-1 (Epitomics Inc., Burlingame, US), polyclonal rabbit anti-human mitogen activated protein kinase (ERK1, ERK2) antibody M-5670 (Sigma, Taufkirchen, Germany), monoclonal mouse anti-human MAP kinase, activated (Diphosphorylated ERK-1&2) antibody M-8159 (Sigma, Taufkirchen, Germany), polyclonal rabbit anti-human Puma antibody (Sigma, Taufkirchen, Germany), polyclonal rabbit anti-human caspase-3 antibody sc-7148 (Santa Cruz, Santa Cruz, US), monoclonal rabbit anti-human caspase-3 antibody (8G10) sc-9665 (Santa Cruz, Santa Cruz, US), monoclonal mouse anti-human PARP antibody (Becton Dickinson, Franklin Lakes, US)).

MST2-kinase activity assay

MST2 immunoprecipitates or cell lysates were separated by SDS-PAGE using gels that were co-polymerised with 0.5mg/ml myelin basic protein (MBP). In-gel kinase assays were performed as described previously (17) except that after the final wash gels were soaked in 50mM Hepes pH7.4, 10mM MgCl₂, 2mM DTT, for 30 minutes prior to the addition of 50µM ATP including 1.85MBq [32P] γ-ATP in a total volume of 10ml.

Apoptosis assays

Attached and floating cells were harvested, washed with PBS, and fixed in 80% ethanol. Subsequently, cells were incubated with RNase A (10U, Roche, Mannheim, Germany) and stained with propidium iodide (50µg/ml) prior to analysis on a FACS flow cytometer (BD Clontech, Heidelberg, Germany). Apoptosis was determined by measuring subgenomic DNA content.

Image analysis and quantification

Relative expression levels from RT-PCRs and immunoblots were assessed using Quantity One software according to the manufacturer's instructions (Biorad, Richmond, USA).

Statistical analysis

Significance levels were determined by two-tailed Student t-test analyses using Microsoft Excel. Due to the non-normal distribution of the expression analysis data (RT-PCR), results are given as the median with the interquartile range (IQR). For comparison of hnRNPH and A-Raf expression between sample groups, we used the Mann-Whitney U-test. The association between hnRNPH expression and the expression of A-Raf was tested using

Pearson correlation. All tests were two-sided and results considered significant if $p < 0.01$. Calculations were carried out with Minitab 15 software (Minitab Ltd., Coventry, UK).

Results

HnRNP H is overexpressed in carcinomas

HnRNP H was over-expressed in head and neck carcinomas, while normal mucosa samples displayed low levels of hnRNP H with the exception of an intermediate expression in cells of the basal membrane layer (Fig. 1). HnRNP H was overexpressed in the vast majority of head and neck carcinoma, *i.e.* in 60% of oropharynx, 80% of hypopharynx, 100% of larynx carcinomas, and 67% of lymph node metastases (Suppl. Table 1). Dysplasia of the head and neck area also showed an increase in hnRNP H expression (data not shown). In normal tissue, hnRNP H was absent or only faintly detectable in most human tissues including muscle, heart, liver, kidney, and pancreas samples. Prostate, gastric, and gut epithelium, as well as spleen and testis cells showed an intermediate expression of hnRNP H as compared with carcinoma samples (Suppl. Fig. S1).

Downregulation of hnRNP H induces apoptosis

Knock-down of hnRNP H in HeLa (cervix), GHD-1 (hypopharynx), and HCT116 (colon) cells *via* RNA interference (Figs. 2a, S2a,b) reduced cell numbers (Fig. 2b) by induction of apoptosis as evidenced by activation of Caspase 3, PARP cleavage, and tenfold increases in DNA fragmentation with up to 50% of cells displaying a pronounced sub-G1 DNA content (Fig. 2a). Decreased cell numbers could be completely rescued by exogenous hnRNP H expression (Suppl. Fig. S2c) and were hence not the result of off-target effects of the siRNAs used. Transient hnRNP H overexpression also protected against etoposide-induced apoptosis by 50% (Fig. 2c), confirming that hnRNP H has anti-apoptotic properties under both normal growth conditions and under cytotoxic drug challenge.

A-Raf and Bcl-x_l are splicing targets of hnRNP H

As hnRNP H is a splicing factor, we performed a genome-wide cDNA microarray screening to profile hnRNP H target mRNAs potentially involved in apoptosis (data not shown). Down-regulation of hnRNP H caused a decrease in anti-apoptotic Bcl-x_l and A-Raf mRNA and protein levels (Figs. 3a,b), which theoretically could promote apoptosis. HnRNP H specifically regulated the expression of wild-type A-Raf, leaving Raf-1 or B-Raf unaffected (Fig. 3b). Transfection of A-Raf, but not Bcl-x_l, prevented apoptosis resulting from hnRNP H repression (Fig. 3c). Double staining of hnRNP H and A-Raf in HNSCC sections and single stainings of consecutive tumour sections revealed a tight correlation between A-Raf and hnRNP H expression, at the single cell level (Fig. 3d, Suppl. Fig. S3a-f).

A-Raf counteracts apoptosis by controlling MST2 activity

To test whether A-Raf mediates hnRNP H apoptosis protection, its expression was suppressed by siRNA (Fig. 4a,b). Knock-down of A-Raf caused a 3-fold reduction in cell numbers (Fig. 4a) and an increase in apoptotic cells similar to the levels observed after hnRNP H inhibition (Fig. 4b). Likewise, A-Raf over-expression counteracted etoposide-mediated apoptosis comparably to hnRNP H (Fig. 4c).

A role in tumour-suppression was suggested for the mammalian MST1/2 kinases, based on their ability to induce cancer cell apoptosis (18-21). Raf-1 suppressed MST2-mediated apoptosis by binding to, and inhibiting the enzymatic activity of MST2, while B-Raf barely interacted with MST2 (17). Transfection of A-Raf inhibited MST2 kinase activity in a dose-dependent fashion (Fig. 5a). In contrast, the knock-down of either hnRNP H or A-Raf augmented MST2 kinase activity, which was fully prevented by complementation with an

A-Raf expression plasmid when knocking down hnRNP H (Fig. 5b). MST kinases are cleaved by caspases, releasing a 36kDa kinase moiety that can translocate to the cell nucleus where it phosphorylates substrates involved in apoptotic processes (18, 22-26). MST2 cleavage and activation of caspase 3 occurred after knock-down of hnRNP H (Suppl. Fig. S4a,b), further confirming that the reduction of hnRNP H expression leads to a critical deregulation of MST2. Additionally, knock-down of either hnRNP H or A-Raf resulted in the activation of caspase 3 and PARP, and an up-regulation of the pro-apoptotic protein Puma (Suppl. Fig. S4a) indicating, that down-stream targets of the MST2 pathway are activated (27). Inhibition of MST2 expression with siRNA fully abrogated apoptosis induced by hnRNP H or A-Raf knock-down, confirming that hnRNP H and A-Raf regulation of apoptosis was MST2-dependent (Fig. 5c).

A-Raf and MST2 interact

Raf-1-mediated inhibition of MST2 effects was dependent on an interaction of both proteins (17). Transfected HA-A-Raf and flag-MST2 as well as endogenous A-Raf and MST2 interacted (Fig. 5d). In addition, A-Raf-K336M, a catalytically inactive mutant, A-Raf-Y301D, a kinase-active mutant, and A-Raf-YY301/302FF, a non-activatable mutant interacted with MST2 similarly as A-Raf (Suppl. Fig. 5a), hence indicating that kinase activity is dispensable for A-Raf's inhibitory effects on MST2. In contrast to the interaction of Raf-1 with MST2, which is disrupted by growth factors [O'Neill, 2004 #18] (Suppl. Fig. 5b), interaction between A-Raf and MST2 revealed largely resistant (Suppl. Fig. 5b). As shown before [O'Neill, 2004 #18], an interaction of the third isoform, B-Raf, with endogenous MST2 is hardly detectable (Suppl. Fig. 5b) and may occur *via* heterodimerisation of B-Raf and Raf-1 (17).

Endogenous localisation of A-Raf and MST2 was visualised in HeLa cells (Suppl. Fig. S6a). Both proteins appeared as cytoplasmic speckles, which perfectly merged in digital overlays (Suppl. Fig. S6b). These speckles represented mitochondria as demonstrated by co-staining with cytochrome C, indicating that A-Raf–MST2 interaction occurs at mitochondria. Importantly, the results obtained in cultured cancer cells were corroborated in human head and neck squamous cell carcinoma (Suppl. Fig. S6c). Similarly, A-Raf and hnRNP H stainings both overlaid with cytochrom C stainings (Suppl. Fig. 6d,e).

hnRNP H and A-Raf are both overexpressed in carcinomas

As suggested from immunohistochemistry with head and neck carcinomas, hnRNP H and A-Raf were both overexpressed in tumours. Next, endogenous mRNA expression levels of hnRNP H and A-Raf were analysed in a series (n=29) of human Dukes B colon carcinomas (T) and autologous adjacent non-malignant tissues (N) by semi-quantitative RT-PCR (Fig. 6a). As a basic principle, hnRNP H and *a-raf* mRNA levels correlated, independently of the tissue analysed. Expression levels of *hnrnpH* and *a-raf* in normal tissue were then set to one for a comparison with the autologous carcinomas. A median relative expression of 2.6-fold for *hnrnpH* and 1.7-fold for *a-raf* in tumour specimens was calculated, indicating that *hnrnpH* and *a-raf* are over-expressed in carcinomas. HnRNP H overexpression significantly correlated with increased levels of A-Raf at the single patient level (Fig. 6b; $r^p=0.564$; $p<0.001$). When patients were divided into three groups according to their relative expression levels of *hnRNP H* and *a-raf* mRNA in tumour tissue (Fig. 6b) a significantly elevated number of patients showed both high expression of *hnRNP H* (n=16/29, $\chi^2=21.8$, $p=0.001$) and *a-raf* (n=11/29, $\chi^2=16.7$, $p=0.001$) (Fig. 6b). Comparing the relative expression of *hnRNP H* and *a-raf* mRNA in normal and tumour tissues (Fig. 6c) we found that in tumour tissues the expression of *hnRNP H* (406 [IQR 278-462]) was significantly higher than in normal tissues (137 [IQR 100-290], $p=0.0001$), corresponding to a 3-fold

increase. Expression of *a-raf* (328 [IQR 174-404]) was also significantly higher than in normal tissue (186 [IQR 138-276], $p=0.0026$), corresponding to a 1.8-fold increase.

Discussion

Tissue homeostasis and tumour-suppression are in part maintained by naturally imposed pro-apoptotic events. Rapidly proliferating cells, including tumour cells, depend on anti-apoptotic signals that counteract intrinsic and extracellular death promoting factors in order to survive (28, 29). Various carcinoma entities present an over-expression of the nuclear factor hnRNP H (11, 12). Here we show that hnRNP H promotes the proper generation of *a-raf* mRNA to express full-length A-Raf protein. As a member of the Raf family, A-Raf was long seen as kinase, though with poor enzymatic potential. As a result of hnRNP H inhibition, an additional variant of *a-raf* mRNA was detectable, which probably represented a shortened, alternatively spliced variant. Whether this shortened mRNA gives rise to a variant A-Raf protein and what functions are assigned to this potential protein remains to be elucidated.

Knowledge of a pathophysiological role of A-Raf in cancer cells is rather scarce when compared to Raf-1 and B-Raf. Especially the comparatively low capacity of A-Raf to phosphorylate MEK, the only widely accepted substrate for Raf kinases, was suggestive of alternative functions of A-Raf (30, 31). Our results suggest that a physiological relevance of maintaining high-level expression of A-Raf is to prevent apoptosis by antagonizing the pro-apoptotic kinase MST2. This pathway has emerged as an important mode of control of apoptosis both in *Drosophila melanogaster*, where the MST2 orthologue is called Hippo (22), and in mammals (18). Downstream MST2 substrates such as Lats and hWW45 (called Warts and Salvador in *Drosophila melanogaster*, respectively) have been identified as tumour suppressor genes in mammals (32). Raf-1 has been shown to interfere with MST2 dimerisation and phosphorylation by directly binding MST2 (17). As a result, MST2-mediated apoptosis was prevented. The B-Raf isoform did not bind MST2 and could not compensate for Raf-1 in this respect (17). Our results show that the third Raf family member, the A-Raf isoform (33), can efficiently repress MST2 activity and induction of apoptosis. Interestingly, this capability depends on the presence of hnRNP H, which enhances the generation of full length A-Raf. MST2 and A-Raf were concomitantly over-expressed and co-localised at mitochondria in cancer cell lines and also in primary human tumours. The significance of this co-localisation at mitochondria warrants further investigation, but may explain why in human cancers A-Raf seems more efficient in inhibiting MST2 pro-apoptotic activity than Raf-1. A role for the potential shortened variant of A-Raf in binding MST2 is as yet unknown. A short isoform of A-Raf might lack the ability to bind to MST-2 and thus might be ineffective in repressing apoptosis.

In mice, A-Raf knock-out resulted in a severe phenotype in X^{-}/Y males and in X^{-}/X^{-} females, hence in homozygous knock-outs as *a-raf* maps to the X-chromosome. Deficient animals died within 7-21 days after birth, displaying abnormalities in colon organogenesis, and neurological defects resulting in abnormal movement and proprioception. Although *in vivo* biochemical evidence is missing, these pathological phenotypes seem reconcilable with increased apoptosis due to a lack of A-Raf control over the MST2 pathway (34, 35). Inhibition of MST2 does neither require Raf-1's (17) nor A-Raf's kinase activity. Such an anti-apoptotic, kinase-independent function would be consistent with a comparably low MEK kinase activity of A-Raf (36) and was corroborated by the interaction of MST2 with a kinase-deficient variant of A-Raf. However, A-Raf still participates in ERK pathway as shown by double knock-outs of Raf-1 and A-Raf in mouse embryos (37), although an inverse correlation between the kinase activity of Raf homologues and the capacity to interact with MST2 emerges from the data available (17).

In summary, our study presents three central findings: (i) A-Raf is a potent inhibitor of MST2-dependent apoptosis; (ii) hnRNP H is necessary for proper splicing of mature A-Raf; and (iii) the hnRNP H–A-Raf–MST2 axis seems instrumental in human tumours.

Supplementary Material

Refer to Web version on PubMed Central for supplementary material.

Acknowledgments

Part of the work was supported by grants from the Deutsche Forschungsgemeinschaft to O.G. and C.M. (GI 540/1-1), the EU FP6 Interaction Proteome grant LSHG-CT-2003-505520 (E.O. and W.K.) and Cancer Research UK (W.K.).

References

- Honore B, Rasmussen HH, Vorum H, et al. Heterogeneous nuclear ribonucleoproteins H, H', and F are members of a ubiquitously expressed subfamily of related but distinct proteins encoded by genes mapping to different chromosomes. *J Biol Chem.* 1995; 270:28780–9. [PubMed: 7499401]
- Chou MY, Rooke N, Turck CW, Black DL. hnRNP H is a component of a splicing enhancer complex that activates a c-src alternative exon in neuronal cells. *Mol Cell Biol.* 1999; 19:69–77. [PubMed: 9858532]
- Garneau D, Revil T, Fisette JF, Chabot B. Heterogeneous nuclear ribonucleoprotein F/H proteins modulate the alternative splicing of the apoptotic mediator Bcl-x. *J Biol Chem.* 2005; 280:22641–50. [PubMed: 15837790]
- Dominguez C, Allain FH. NMR structure of the three quasi RNA recognition motifs (qRRMs) of human hnRNP F and interaction studies with Bcl-x G-tract RNA: a novel mode of RNA recognition. *Nucleic Acids Res.* 2006; 34:3634–45. [PubMed: 16885237]
- Wang E, Dimova N, Cambi F. PLP/DM20 ratio is regulated by hnRNPH and F and a novel G-rich enhancer in oligodendrocytes. *Nucleic Acids Res.* 2007; 35:4164–78. [PubMed: 17567613]
- Kalifa Y, Huang T, Rosen LN, Chatterjee S, Gavis ER. Glorund, a Drosophila hnRNP F/H homolog, is an ovarian repressor of nanos translation. *Dev Cell.* 2006; 10:291–301. [PubMed: 16516833]
- Schaub MC, Lopez SR, Caputi M. Members of the heterogeneous nuclear ribonucleoprotein H family activate splicing of an HIV-1 splicing substrate by promoting formation of ATP-dependent spliceosomal complexes. *J Biol Chem.* 2007; 282:13617–26. [PubMed: 17337441]
- Chen CD, Kobayashi R, Helfman DM. Binding of hnRNP H to an exonic splicing silencer is involved in the regulation of alternative splicing of the rat beta-tropomyosin gene. *Genes Dev.* 1999; 13:593–606. [PubMed: 10072387]
- Grabowski PJ. A molecular code for splicing silencing: configurations of guanosine-rich motifs. *Biochem Soc Trans.* 2004; 32:924–7. [PubMed: 15506926]
- Martinez-Contreras R, Fisette JF, Nasim FU, Madden R, Cordeau M, Chabot B. Intronic binding sites for hnRNP A/B and hnRNP F/H proteins stimulate pre-mRNA splicing. *PLoS Biol.* 2006; 4:e21. [PubMed: 16396608]
- Honore B, Baandrup U, Vorum Hw. Heterogeneous nuclear ribonucleoproteins F and H/H' show differential expression in normal and selected cancer tissues. *Exp Cell Res.* 2004; 294:199–209. [PubMed: 14980514]
- Rauch J, Ahlemann M, Schaffrik M, et al. Allogenic antibody-mediated identification of head and neck cancer antigens. *Biochem Biophys Res Commun.* 2004; 323:156–62. [PubMed: 15351715]
- Hsu SM, Raine L, Fanger H. The use of antiavidin antibody and avidin-biotin-peroxidase complex in immunoperoxidase technics. *Am J Clin Pathol.* 1981; 75:816–21. [PubMed: 6167159]
- Mayer A, Andratschke M, Pauli C, Graefe H, Kristina K, Wollenberg B. Generation of an autologous cell system for immunotherapy of squamous cell carcinoma of the head and neck. *Anticancer Res.* 2005; 25:4075–80. [PubMed: 16309201]

15. ImageJ. <http://rsbinfo.nih.gov/ij/>
16. Schneider C, Newman RA, Sutherland DR, Asser U, Greaves MF. A one-step purification of membrane proteins using a high efficiency immunomatrix. *J Biol Chem.* 1982; 257:10766–9. [PubMed: 6955305]
17. O'Neill E, Rushworth L, Baccharini M, Kolch W. Role of the kinase MST2 in suppression of apoptosis by the proto-oncogene product Raf-1. *Science.* 2004; 306:2267–70. [PubMed: 15618521]
18. O'Neill EE, Matallanas D, Kolch W. Mammalian sterile 20-like kinases in tumor suppression: an emerging pathway. *Cancer Res.* 2005; 65:5485–7. [PubMed: 15994916]
19. Jia J, Zhang W, Wang B, Trinko R, Jiang J. The Drosophila Ste20 family kinase dMST functions as a tumor suppressor by restricting cell proliferation and promoting apoptosis. *Genes Dev.* 2003; 17:2514–9. [PubMed: 14561774]
20. Pantalacci S, Tapon N, Leopold P. The Salvador partner Hippo promotes apoptosis and cell-cycle exit in Drosophila. *Nat Cell Biol.* 2003; 5:921–7. [PubMed: 14502295]
21. Harvey KF, Pflieger CM, Hariharan IK. The Drosophila Mst ortholog, hippo, restricts growth and cell proliferation and promotes apoptosis. *Cell.* 2003; 114:457–67. [PubMed: 12941274]
22. O'Neill E, Kolch W. Taming the Hippo: Raf-1 controls apoptosis by suppressing MST2/Hippo. *Cell Cycle.* 2005; 4:365–7. [PubMed: 15701972]
23. Graves JD, Gotoh Y, Draves KE, et al. Caspase-mediated activation and induction of apoptosis by the mammalian Ste20-like kinase Mst1. *Embo J.* 1998; 17:2224–34. [PubMed: 9545236]
24. Lee KK, Ohyama T, Yajima N, Tsubuki S, Yonehara S. MST, a physiological caspase substrate, highly sensitizes apoptosis both upstream and downstream of caspase activation. *J Biol Chem.* 2001; 276:19276–85. [PubMed: 11278283]
25. Kakeya H, Onose R, Osada H. Activation of a 36-kD MBP kinase, an active proteolytic fragment of MST/Krs proteins, during anticancer drug-induced apoptosis. *Ann N Y Acad Sci.* 1999; 886:273–5. [PubMed: 10667237]
26. Watabe M, Kakeya H, Onose R, Osada H. Activation of MST/Krs and c-Jun N-terminal kinases by different signaling pathways during cytotrienin A-induced apoptosis. *J Biol Chem.* 2000; 275:8766–71. [PubMed: 10722720]
27. Matallanas D, Romano D, Yee K, et al. RASSF1A elicits apoptosis through an MST2 pathway directing proapoptotic transcription by the p73 tumor suppressor protein. *Mol Cell.* 2007; 27:962–75. [PubMed: 17889669]
28. Green DR. Apoptotic pathways: ten minutes to dead. *Cell.* 2005; 121:671–4. [PubMed: 15935754]
29. Hanahan D, Weinberg RA. The hallmarks of cancer. *Cell.* 2000; 100:57–70. [PubMed: 10647931]
30. Dhillon AS, Hagan S, Rath O, Kolch W. MAP kinase signalling pathways in cancer. *Oncogene.* 2007; 26:3279–90. [PubMed: 17496922]
31. Dhillon AS, Kolch W. Oncogenic B-Raf mutations: crystal clear at last. *Cancer Cell.* 2004; 5:303–4. [PubMed: 15093535]
32. Tapon N, Harvey KF, Bell DW, et al. salvador Promotes both cell cycle exit and apoptosis in Drosophila and is mutated in human cancer cell lines. *Cell.* 2002; 110:467–78. [PubMed: 12202036]
33. Baccharini M. An old kinase on a new path: Raf and apoptosis. *Cell Death Differ.* 2002; 9:783–5. [PubMed: 12107820]
34. Pritchard CA, Bolin L, Slattery R, Murray R, McMahon M. Post-natal lethality and neurological and gastrointestinal defects in mice with targeted disruption of the A-Raf protein kinase gene. *Curr Biol.* 1996; 6:614–7. [PubMed: 8805280]
35. Hagemann C, Rapp UR. Isotype-specific functions of Raf kinases. *Exp Cell Res.* 1999; 253:34–46. [PubMed: 10579909]
36. Marais R, Light Y, Paterson HF, Mason CS, Marshall CJ. Differential regulation of Raf-1, A-Raf, and B-Raf by oncogenic ras and tyrosine kinases. *J Biol Chem.* 1997; 272:4378–83. [PubMed: 9020159]

37. Mercer K, Giblett S, Oakden A, Brown J, Marais R, Pritchard C. A-Raf and Raf-1 work together to influence transient ERK phosphorylation and G1/S cell cycle progression. *Oncogene*. 2005; 24:5207–17. [PubMed: 15856007]

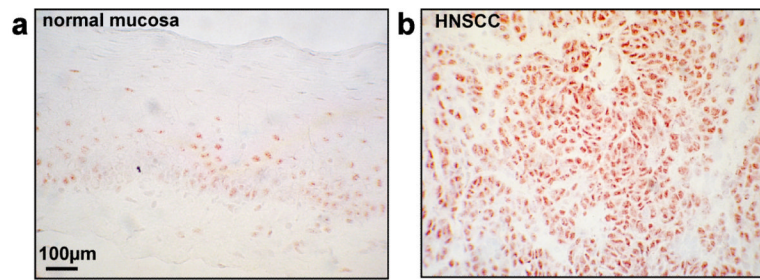


Figure 1. hnRNP H is overexpressed in HNSCC

HnRNP H expression was detected in normal mucosa (a) and carcinoma tissue (b) (HNSCC). Immunohistochemistry was performed on cryosections of human tissue specimens.

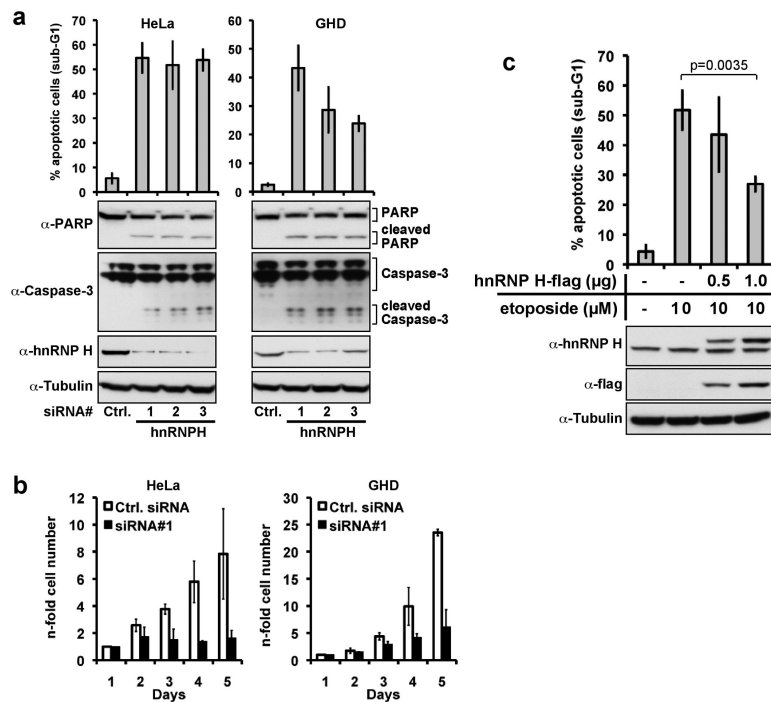


Figure 2. Knock-down of hnRNP H induces apoptosis in carcinoma cell lines

(a) HeLa cells and GHD cells were transfected with with three different hnRNP H specific siRNA oligonucleotides (siRNA#1-3) or scrambled control siRNA (Ctrl. siRNA) at 100nM final concentration. Three days after transfection, apoptosis was measured by flow cytometry assessing fragmented DNA content (subG1) (upper panel). Additionally, cells were lysed, and expression of hnRNP H, Caspase-3, and PARP was assessed by immunoblotting (lower panels). Shown are mean values with SD from three independent experiments. (b) Numbers of HeLa and GHD-1 cells were determined in a time kinetic following siRNA#1 (black bars), or control siRNA (open bars) transfection. Results represent the mean with standard deviation (SD) of three independent experiments. (c) HnRNP H overexpression partly counteracts etoposide-induced apoptosis. HeLa cells were transfected with indicated amounts of a hnRNP H expression plasmid, and treated with 10μM etoposide 24 hours later. 72 hours post transfection the proportion of apoptotic cells was assessed by measuring DNA fragmentation by flow cytometry. Shown are mean values with SD from three independent experiments (upper panel). Additionally, cells were lysed, and hnRNP H- and flag- expression was assessed by immunoblotting (lower panel).

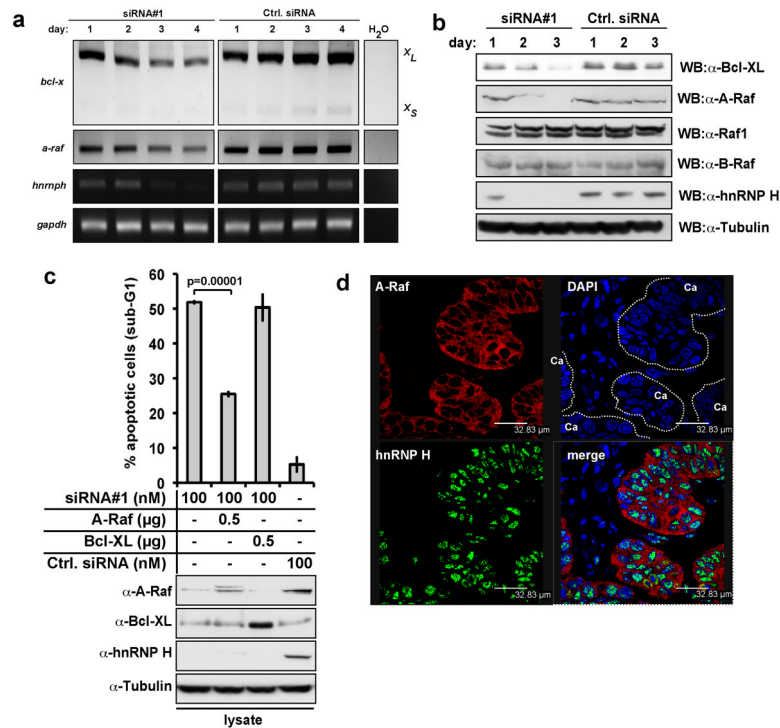


Figure 3. hnRNP H controls *bcl-x* and *a-raf* mRNA levels and splicing, but only A-Raf antagonises apoptosis induced by hnRNP H depletion

(a) *bcl-x*_{L/S}, *a-raf*, and *hnRNP H* mRNA expression in HeLa cells was analyzed by semi-quantitative RT-PCR four days after transfection with control (Ctrl. siRNA) or hnRNP H-specific siRNA (siRNA#1). *gapdh* mRNA levels were determined as loading controls. Shown is a representative result from three independent experiments. (b) Bcl-x_L, A-Raf, Raf-1, B-Raf and hnRNP H protein expression was analyzed by immunoblotting three days post-transfection with control (Ctrl. siRNA) or hnRNP H-specific siRNA (siRNA#1). As loading control tubulin protein levels were determined. Shown are representative results from three independent experiments. (c) HeLa cells were co-transfected with A-Raf or Bcl-x_L expression plasmids and siRNAs as indicated. Apoptosis was determined assessing DNA fragmentation by flow cytometry three days post-transfection. The data represent mean percentage of apoptosis with SD of three independent experiments (upper panel). hnRNP H-, A-Raf- and Bcl-x_L-expression was assessed by immunoblotting (lower panel). (d) HnRNP H and A-Raf co-localise in primary carcinomas. HnRNP H and A-Raf were visualized using double staining with the respective antibodies.

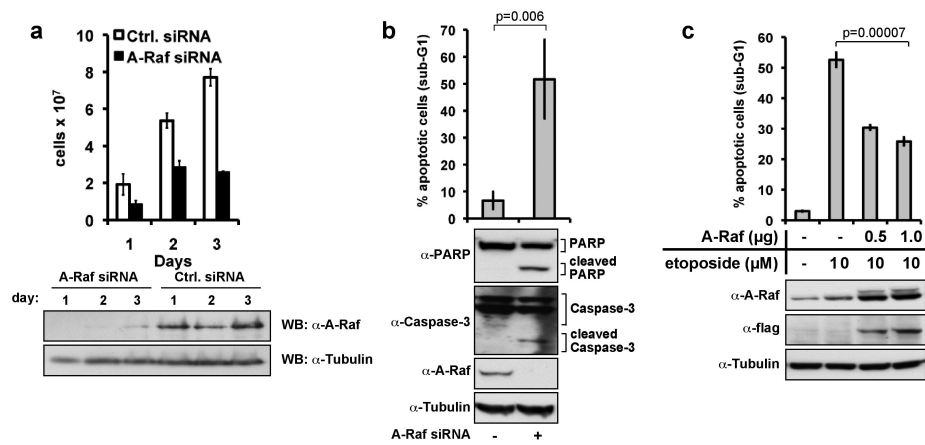


Figure 4. A-Raf mediates carcinoma cell survival

(a) HeLa cells were transfected with 100nM A-Raf siRNA oligonucleotides or control siRNA. Cell numbers were assessed at the indicated time points after transfection with A-Raf or control siRNAs. Shown are mean values with SD from two independent experiments. In parallel, the expression of A-Raf was monitored in whole cell lysates for three days post transfection by immunoblotting. Shown are representative results from three independent experiments (lower panels). **(b)** Apoptosis was assessed by DNA fragmentation three days after transfection with A-Raf or control siRNAs. Shown are mean values with SD from three independent experiments. Additionally, cells were lysed, and expression of A-Raf, Caspase-3, and PARP was assessed by immunoblotting (lower panels). **(c)** A-Raf overexpression counteracts etoposide-induced apoptosis. HeLa cells were transfected with increasing amounts of an A-Raf expression plasmid (flag-tagged A-Raf), and treated with 10μM etoposide 24 hours later. 72 hrs post transfection the proportion of apoptotic cells was assessed upon measuring DNA fragmentation by flow cytometry (upper panel). Shown are mean values with SD from three independent experiments. In parallel, the expression of A-Raf was monitored in whole cell lysates by immunoblotting (lower panel).

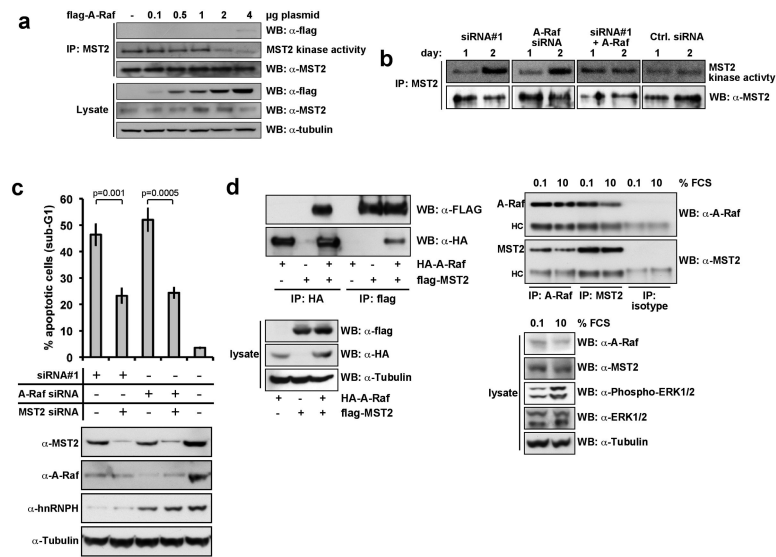


Figure 5. HnRNP H and A-Raf suppress apoptosis via inhibition of MST2 kinase activation
(a) Increasing amounts of Flag-A-Raf expression plasmids were transiently transfected into HEK293 cells, and MST2 immunoprecipitates were examined for kinase activity using an in-gel kinase assay. An equal aliquot was used for immunoblotting to assure that equal amounts of MST2 had been immunoprecipitated. Lysates were immunoblotted for expression of the transfected Flag-A-Raf and tubulin as loading control. Shown are the representative results from three independent experiments. **(b)** HeLa cells were transiently transfected with hnRNP H (siRNA#1), A-Raf, and control siRNAs at final concentrations of 100nM. Where indicated, A-Raf expression plasmid (1.0µg) was co-transfected. The kinase activity of MST2 immunoprecipitates was assessed by in-gel kinase assays at day one and two after transfection (upper panel). The amount of MST2 immunoprecipitated from whole cell lysates was visualized by immunoblotting (lower panel). **(c)** HeLa cells were transfected with hnRNP H siRNA, A-Raf siRNA or MST2 siRNA as indicated. Total amounts of siRNA were adjusted using control siRNA. Three days post transfection apoptosis was determined by assessing DNA fragmentation using flow cytometry. Shown are mean values with SD from three independent experiments (upper panel). In parallel, the expression of hnRNP H, A-Raf, and MST2 was monitored in whole cell lysates by immunoblotting (lower panel). **(d) A-Raf and MST2 interact in cultured cells.** (left panel) Flag-tagged MST2 and HA-tagged A-Raf were transiently transfected in HEK293 cells. After 24hrs MST2 and A-Raf were immunoprecipitated (IP) with flag-tag or HA-tag specific antibodies, and analysed by immunoblotting (WB) (upper panel). Lysates were immunoblotted for expression of the transfected HA-A-Raf, flag-tagged MST2 and tubulin as loading control (lower panel) (right panel) Endogenous A-Raf and MST2 were immunoprecipitated from lysates of HeLa cells, which had been serum starved (0.1% FCS, 16 hours) or treated full medium (10% FCS) after serum-starvation using specific antibodies for A-Raf or MST2, and analysed by immunoblotting. As an isotype control an antibody specific for Enolase was used (upper panel). Lysates were immunoblotted for expression of A-Raf, MST2, phosphorylated ERK1/2, ERK1/2, and tubulin as loading control (lower panel). HC – heavy chain immunoglobulin. Shown are the representative results from three independent experiments.

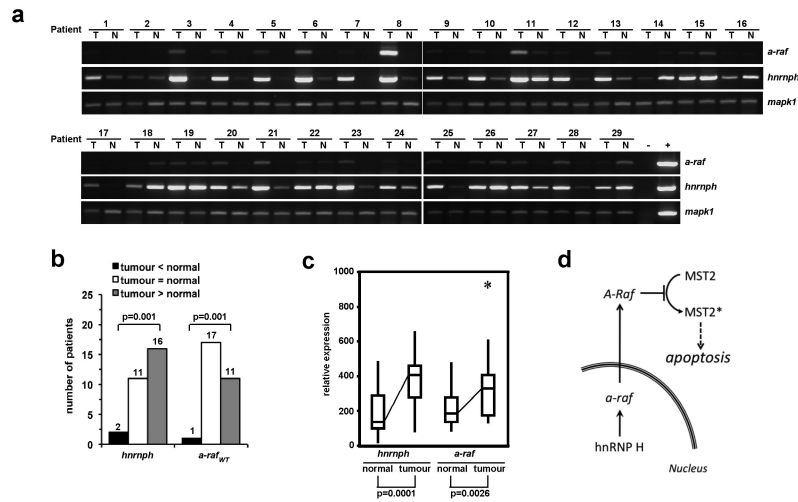


Figure 6. Expression of *hnRNP H* and *a-raf* in colon carcinomas and normal adjacent tissues
(a) The expression of *hnRNP H* and *a-raf* mRNA was assessed in colon tumours (T) and normal adjacent tissues (N) by semi-quantitative RT-PCR as described in materials and methods. *Mapk1* mRNA levels were determined as a loading control. **(b) Significantly elevated number of patients with high expression of *hnRNP H* and *a-raf* in tumours.** The expression level of *hnRNP H* and *a-raf* in tumour tissue was correlated to each corresponding normal tissue after standardization of all values using *mapk1*. Patients were divided into three groups according to their relative expression levels of *hnRNP H* and *a-raf* mRNA in tumour tissue. Black bars (tumour < normal) indicate tissues where expression in the tumour is lower than in normal tissues, white bars (tumour = normal) indicate no significant difference between normal and tumour tissue, and grey bars (tumour > normal) indicate tissues where expression in the tumour is significantly higher than in normal tissues. Shown are the numbers of patients in each group. The distribution of relative expression was calculated using the Chi-square test. **(c)** Relative expression of *hnRNP H* and *a-raf* mRNA according to disease state of the tissue. Significantly elevated expressions of *hnRNP H* and *a-raf* were observed in tumour tissues. Shown are boxplots where boxes indicate the median (line) and IQR, whiskers show the range, and asterisks indicate outliers. **(d) Model for HnRNP H-mediated A-Raf transcription and regulation of MST2-Dependent Apoptosis.** hnRNP H is necessary for proper splicing of mature A-Raf. A-Raf binds to MST2 and thus, is a potent inhibitor of MST2-dependent apoptosis.